

Double Lactonization in Triarylamine-Conjugated Dimethyl Diethynylfumarate: Formation of Intensely Colored and Luminescent Quadrupolar Molecules Including a Missing Structural Isomer of Pechmann Dyes

Mikihiro Hayashi, Fumiyuki Toshimitsu, Ryota Sakamoto, and Hiroshi Nishihara*

Department of Chemistry, Graduate School of Science, The University of Tokyo, 7-3-1 Hongo, Bunkyo-ku, Tokyo 113-0033, Japan

S Supporting Information

ABSTRACT: Acid-induced double lactonization in triarylamine-conjugated dimethyl diethynylfumarate *E-1* opens up a new synthetic route to Pechmann dyes. This one-pot reaction affords three donor–acceptor–donor quadrupolar molecules (*P*₅₅-**1**, *P*₆₆-**1**, and *P*₅₆-**1**); *P*₅₆-**1** comprises a missing structural isomer of Pechmann dyes. They are intensely colored and brightly luminescent. An organic field-effect transistor device fabricated with *P*₆₆-**1** functions as a p-type semiconductor.

D–A–D and A–D–A (D = donor, A = acceptor) types of molecules feature strong one-photon absorptions in the visible and NIR regions, which are assigned as intramolecular charge-transfer (ICT) transitions; their large absorptivities often lead to high fluorescence quantum yields.¹ On the other hand, it has been demonstrated that these types of molecules possess gigantic two-photon absorption cross sections, which stem from drastic changes in their quadrupole moment upon photoexcitation.² Because of these valuable photoproperties, D–A–D and A–D–A “quadrupolar” molecules have received great attention for their use in bioimaging,³ photodynamic therapy (PDT),⁴ optical power limiting,⁵ organic light-emitting diodes (OLEDs),⁶ organic photovoltaic devices (OPVs),⁷ and so on. Recently, organic field-effect transistors (OFETs) based on quadrupolar molecules have also been reported.⁸

Using our original acceptor framework, dimethyl diethynylfumarate,^{9,10} we created the unique D–A–D quadrupolar system *E-1* (Scheme 1) in combination with triarylamine (TAA) donors. *E-1* was found to be intensely colored and luminescent, and it underwent reversible visible-light photoisomerization to produce ON/OFF luminescence switching as well as modulation of the electronic communication between the TAA cores in the one-electron-oxidized mixed-valent (MV) state.^{9,10}

Pechmann dyes (Scheme 2) are good pigments and acceptors featuring rigid, planar structures that stem from the cross-conjugated, electron-withdrawing lactone rings.¹¹ These properties are optimal for the construction of D–A–D quadrupolar molecules having intense D–A interactions and large effective intermolecular overlaps in the solid state; however, the Pechmann dye frameworks have not been sufficiently appreciated in D–A chemistry.

Several synthetic routes to the Pechmann dye family are available. For example, dehydrative dimerization of β -aroylacrylic

acid gives rise to the 5,5-membered isomer (*P*₅₅), which undergoes thermal isomerization to give the 6,6-membered isomer (*P*₆₆) (Scheme 2).¹¹ However, no route to other structural isomers, such as the 5,6- and 5,5-membered frameworks (*P*₅₆ and *P*_{55'}, respectively), have been established to date.

As Yamaguchi and co-workers illustrated, intramolecular double cyclization is a valuable tool for the creation of functional molecules that feature high planarity, a fused-ring structure, and intensive π conjugation.¹² We regard the dimethyl diethynylfumarate framework as an open form of Pechmann dyes protected by the methyl ester groups, and we expect that with an appropriate ring-closure reaction, it can open up a new route to the Pechmann dye family and provide access to their missing structural isomers.

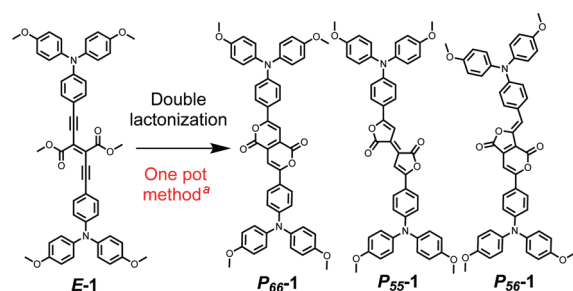
In this communication, we disclose a new synthetic method for Pechmann dyes via novel acid-induced double lactonization (Scheme 1). Application of this method to TAA-appended *E-1* produced in one-pot the three D–A–D quadrupolar molecules *P*₆₆-**1**, *P*₅₅-**1**, and *P*₅₆-**1** (Scheme 1), the last of which constitutes one of the missing structural isomers of the Pechmann dye family (*P*₅₆ in Scheme 2). We demonstrate that *P*₆₆-**1**, *P*₅₅-**1**, and *P*₅₆-**1** show more intense D–A interactions than the parent *E-1*: all exhibit greater and red-shifted ICT bands and brighter fluorescence. The performance of an OFET device made of *P*₆₆-**1** is also briefly described.

Treatment of *E-1* with a mixture of concentrated hydrochloric acid and glacial acetic acid afforded three intensely colored compounds that were separated by column chromatography on silica gel. The three compounds had identical molecular weights as detected by high-resolution fast atom bombardment mass spectrometry but gave different ¹H NMR [Figure 1a and Figures S1–S3 in the Supporting Information] and ¹³C NMR (Figures S4–S6) spectra. These three compounds were successfully characterized by single-crystal X-ray structure analysis, which identified them as *P*₅₅-**1**, *P*₆₆-**1**, and *P*₅₆-**1** (Figure 1b and Figure S7). We note that the fused-ring structure of *P*₅₆-**1**, which is one of the isomeric forms of Pechmann dyes, has not been reported previously. A proposed reaction mechanism is illustrated in Scheme 3. First, *E-1* undergoes de-esterification to produce the corresponding fumaric acid. Next, the first nucleophilic cyclization between the carboxyl group and ethynylene proceeds. When the ethynylene on the α carbon to the carboxyl

Received: June 11, 2011

Published: August 15, 2011

Scheme 1. Double Lactonization in *E*-1 and the Three Resultant Triarylamine-Appended Pechmann Dyes



^a Conditions: AcOH/HCl, under N₂, reflux. See the Supporting Information for detailed reaction conditions.

Scheme 2. Pechmann Dye Frameworks (The Fused-Ring Structures of *P*₅₆ and *P*₅₅ Have Not Been Reported Previously)

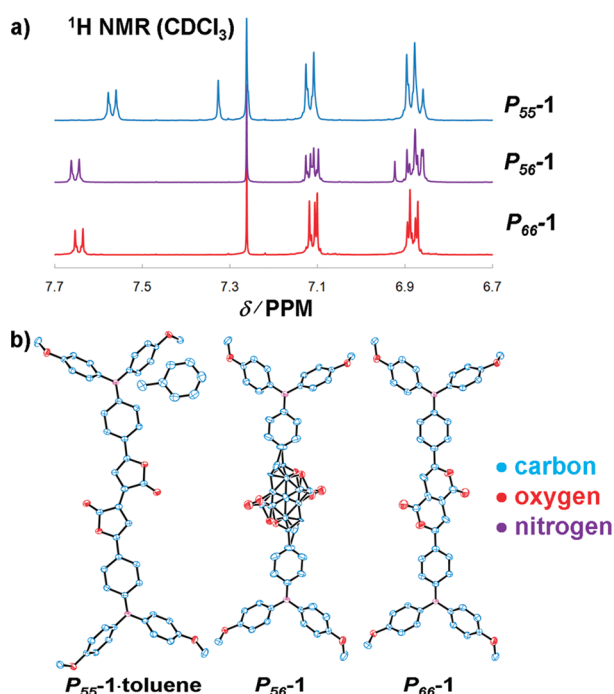
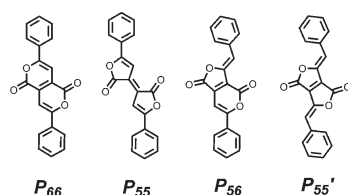


Figure 1. (a) ¹H NMR spectra in the aromatic region for *P*₅₅-1, *P*₅₆-1, and *P*₆₆-1 in CDCl₃. (b) ORTEP drawings of *P*₅₅-1·toluene, *P*₅₆-1, and *P*₆₆-1 with thermal ellipsoids at the 50% probability level. H atoms have been omitted. Two conformations are disordered with respect to the fused-ring moiety of *P*₅₆-1 (see Figure S7 for a detailed explanation of this disorder).

group participates in the cyclization, *P*₅₅-1 is generated exclusively via the second annulation. On the other hand, when the

Scheme 3. Plausible Reaction Mechanism of Double Lactonization in *E*-1 (R = Triarylamino Group)

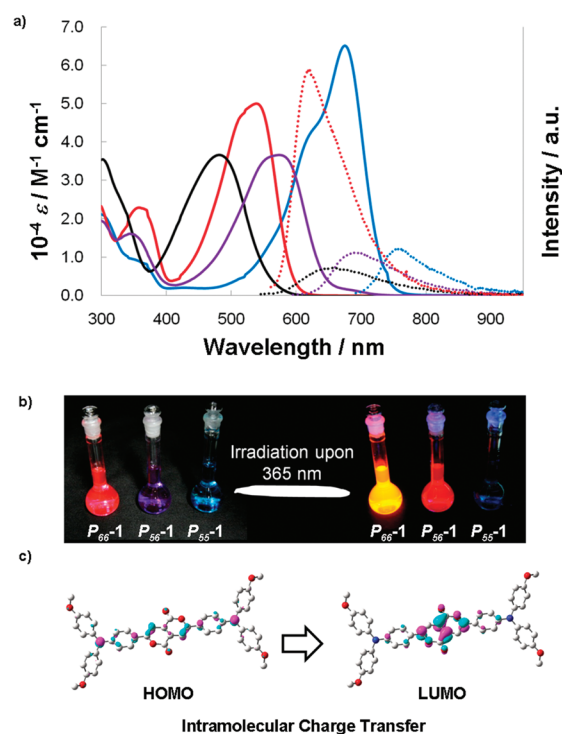
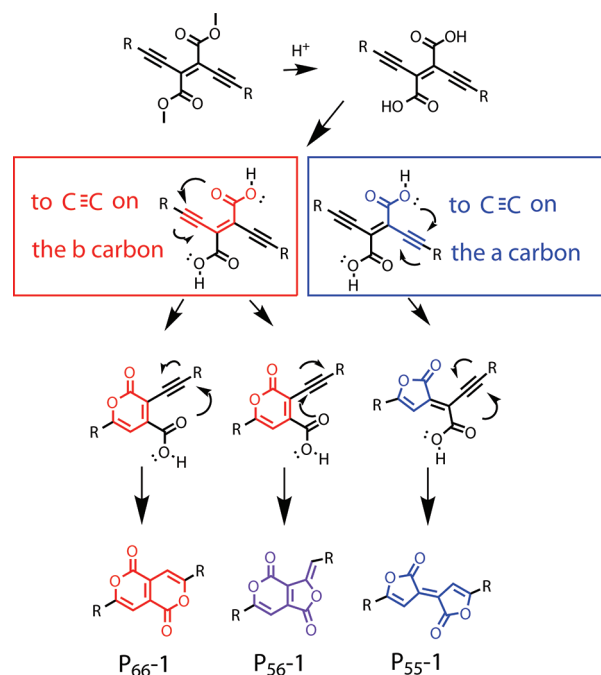
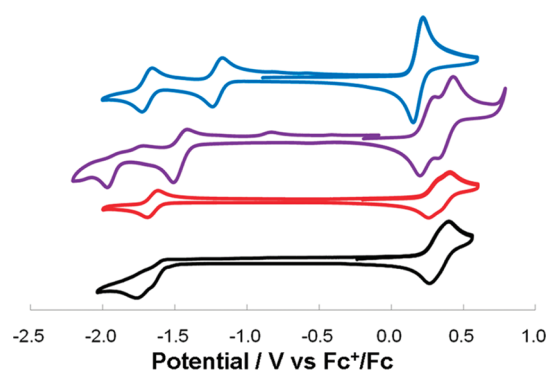


Figure 2. (a) UV-vis-NIR (solid) and fluorescence (dotted) spectra of *P*₅₅-1 (blue), *P*₆₆-1 (red), *P*₅₆-1 (purple), and *E*-1 (black) in toluene. (b) Photograph showing *P*₆₆-1, *P*₅₆-1, and *P*₅₅-1 in toluene under (left) ambient-light and (right) black-light (365 nm) illumination. (c) Molecular orbitals of *P*₆₆-1 involved in the ICT band.

ethynylene on the β carbon is involved in the first annulation, either *P*₆₆-1 or *P*₅₆-1 is produced via the following lactonization.

Table 1. Photochemical Properties of P_{66-1} , P_{55-1} , P_{56-1} , and $E-1$

compound	absorption		fluorescence				
	λ_{\max}	$10^{-4}\epsilon/\text{M}^{-1}\text{cm}^{-1}$	λ_{\max}	Φ	τ/ns	$10^{-9}k_r/\text{s}^{-1}$	$10^{-9}k_{nr}/\text{s}^{-1}$
P_{66-1}	538	5.0	617	0.82	3.0	0.27	0.060
P_{55-1}	674	6.5	753	0.27	1.3	0.21	0.56
P_{56-1}	574	3.7	692	0.20	1.0	0.20	0.80
$E-1$	482	3.6	660	0.15	0.9	0.17	0.94

**Figure 3.** Cyclic voltammograms of P_{55-1} (blue), P_{56-1} (purple), P_{66-1} (red), and $E-1$ (black) in 0.1 M $\text{Bu}_4\text{NBF}_4/\text{CH}_2\text{Cl}_2$ at a sweep rate of 100 mV s^{-1} .

The thermal stabilities of P_{66-1} , P_{56-1} , P_{55-1} , and $E-1$ were examined by thermogravimetric analysis (TGA). Among these, P_{66-1} featured the highest stability, decomposing above 400°C . The thermal stability followed the order $P_{66-1} > P_{56-1} > P_{55-1} > E-1$ (Figure S8).

Figure 2a shows UV–vis–NIR and fluorescence spectra of P_{55-1} , P_{66-1} , and P_{56-1} as well as the parent $E-1$ in toluene; their numerical data are collected in Table 1, and photos of the annulated compounds are shown in Figure 2b. Relative to $E-1$, the cyclized compounds possess more intense and red-shifted absorptions in the visible and NIR regions. We had already identified the visible absorption of $E-1$ as a HOMO–LUMO ICT from the D sites, TAA(n), to the A site, dimethyl diethynylfumarate(π^*).⁹ In the present work, time-dependent density functional theory (TDDFT) calculations for the lactonized compounds were newly conducted and also assigned this series of bands to D–A ICT transitions from TAA(n) to the Pechmann dye framework(π^*) (Figure 2c for P_{66-1} , Figure S9a for P_{55-1} , and Figure S9b for P_{56-1}). Therefore, the cyclized compounds feature narrower HOMO–LUMO gaps, or more intense D–A interactions, than the parent $E-1$. All of the compounds are brightly fluorescent in the visible and NIR regions. The fluorescence quantum yields (Φ) are greater in the annulated P_{66-1} , P_{55-1} , and P_{56-1} than in the parent $E-1$; in particular, P_{66-1} exhibits by far the highest value. The cyclized compounds feature smaller Stokes shifts than $E-1$, which stems from the rigidity of the Pechmann dye frameworks and the flexibility of the photoisomerizable dimethyl diethynylfumarate skeleton.¹³ Transient fluorescence measurements disclosed that the emission lifetimes (τ) were on the order of nanoseconds, and the enhancement of Φ in the cyclized compounds is derived from the deceleration of the nonradiative processes (k_{nr}) rather than the acceleration of the radiative ones (k_r , Table 1 and Figure S10).

Table 2. Electrochemical Properties of P_{66-1} , P_{55-1} , P_{56-1} , and $E-1$ in 0.1 M $\text{Bu}_4\text{NBF}_4/\text{CH}_2\text{Cl}_2$

compound	reduction		oxidation	
	E°/V	$E^{\circ}(1)/\text{V}$	$E^{\circ}(2)/\text{V}$	$\Delta E^{\circ}/\text{mV}^a$
P_{66-1}	−1.69	0.29	0.38	92
P_{55-1}	−1.24	0.18	0.20	23
P_{56-1}	−1.48	0.23	0.47	240
$E-1$	−1.76 ^b	0.29	0.36	72

^a $\Delta E^{\circ} = E^{\circ}(2) - E^{\circ}(1)$. ^b Cathodic peak potential.

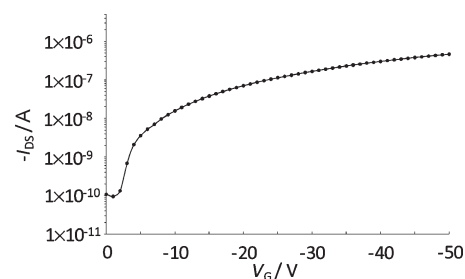
**Figure 4.** Transfer plot for an OFET device fabricated using P_{66-1} ($V_{\text{DS}}, -50\text{ V}$; channel length, $50\text{ }\mu\text{m}$; channel width, 3 cm).

Figure 3 shows cyclic voltammograms for all of the compounds, and their numerical data are gathered in Table 2. All of the cyclized compounds feature at least one reversible one-electron reduction at relatively positive potentials, whereas $E-1$ exhibits an irreversible reduction at a more negative potential. These data indicate that the Pechmann dye frameworks are better acceptors than the parental dimethyl diethynylfumarate. All compounds show reversible oxidations derived from the two TAA moieties. We had previously reported that $E-1$ showed a split in the E° values (ΔE°) for the oxidations of the two TAA moieties, which had been associated with electronic communication between the two TAAs in the MV state $E-1^+$.⁹ Among the three cyclized compounds, the largest ΔE° was observed for P_{56-1} (240 mV), reflective of the different chemical environments of the two TAAs (as clarified by single-crystal X-ray structure analysis; Figure 2b and Figure S7) rather than intense electronic communication. The second largest ΔE° was found for P_{66-1} (92 mV), which was quantified by simulation of the voltammogram (Figure S11a). ΔE° for P_{66-1} is greater than for $E-1$ (74 mV). This difference indicates that the P_{66} ring structure is a better communicator than the dimethyl diethynylfumarate framework. On the other hand, P_{55-1} showed the smallest ΔE° of 23 mV (Figure S11b).

To demonstrate the utility of the cyclized compounds, we investigated a preliminary OFET device based on P_{66-1} , which

displayed the best thermal stability. A top-contact OFET (Figure S12) was fabricated by vacuum evaporation of **P₆₆-1** onto a silicon substrate modified with hexamethyldisilazane (HMDS). The resultant thin film of **P₆₆-1** had a thickness of ~50 nm and served as a p-type semiconductor; Figure 4 shows a transfer plot for the OFET device under air. The maximum hole mobility was calculated to be $5.6 \times 10^{-5} \text{ cm}^2 \text{ V}^{-1} \text{ s}^{-1}$ (Figure S13). The carrier mobility could be enhanced by improving the low crystallinity of the **P₆₆-1** thin film (Figure S14).

In conclusion, we have found a new one-pot reaction for constructing the Pechmann dye framework that involves double lactonization of dimethyl diethynylfumarate under acidic conditions. Here TAA-conjugated **E-1** was used as the starting material, and **P₅₆-1** with a novel 5,6-membered fused-ring structure (one of the missing Pechmann dye isomers) was obtained along with **P₆₆-1** and **P₅₅-1** having known 6,6- and 5,5-membered ring structures, respectively. The three resultant doubly annulated compounds constitute quadrupolar D–A–D systems; photochemical and electrochemical analyses disclosed that they engaged in intense D–A interactions that yielded valuable photoproperties, such as highly intense and red-shifted visible and NIR absorptions and fluorescence. The cyclized compounds also featured high Φ . The thermal durability of the cyclized compounds was superior to that of the parent **E-1**. An OFET device made of the most thermally stable material, **P₆₆-1**, was fabricated by the sublimation method and revealed that **P₆₆-1** acted as a p-type semiconductor. This new methodology for producing the Pechmann dye frameworks is currently being expanded in pursuit of the other missing structure (**P₅₅'** in Scheme 2) as well as control over the selectivity among the isomers, and the methodology is also being applied to starting materials with other donor moieties.

■ ASSOCIATED CONTENT

S Supporting Information. Experimental details; full characterization data for **P₆₆-1**, **P₅₅-1**, and **P₅₆-1** (^1H and ^{13}C NMR spectra and structural analysis of **P₅₆-1**); thermal stability test results for all compounds; TDDFT calculation results for **P₅₅-1** and **P₅₆-1**; simulation of cyclic voltammograms of **P₆₆-1** and **P₅₅-1**; information on the OFET device based on **P₆₆-1**; complete refs 2a and 2c; and crystallographic data (CIF). This material is available free of charge via the Internet at <http://pubs.acs.org>.

■ AUTHOR INFORMATION

Corresponding Author

nishihara@chem.s.u-tokyo.ac.jp

■ ACKNOWLEDGMENT

The authors acknowledge Grants-in-Aid from MEXT of Japan (20245013 and 21108002, Area 2107, Coordination Programming) and the Global COE Program for Chemistry Innovation for financial support. The authors are grateful to Dr. Murata, Dr. Ishii, and Mr. Hirata (Sony Inc.) for assistance with the fabrication and performance evaluation of the OFET device. The authors also thank Dr. Kimiko Hasegawa of Rigaku Corporation for technical support in the X-ray crystallographic analysis. The authors express gratitude to Hamamatsu Photonics K.K. for the fluorescence lifetime measurements with a Quantaurus-Tau fluorospectrometer.

■ REFERENCES

- (1) Susumu, K.; Fisher, J. A. N.; Zheng, J.; Beratan, D. N.; Yodh, A. G.; Therien, M. J. *J. Phys. Chem. A* **2011**, *115*, 5525–5539.
- (2) (a) Albota, M.; et al. *Science* **1998**, *281*, 1653–1656. (b) He, G. S.; Tan, L.-S.; Zheng, Q.; Prasad, P. N. *Chem. Rev.* **2008**, *108*, 1245–1330. (c) Entwistle, C. D.; et al. *J. Mater. Chem.* **2009**, *19*, 7532–7544.
- (3) (a) Didier, P.; Ulrich, G.; Mely, Y.; Ziessel, R. *Org. Biomol. Chem.* **2009**, *7*, 3639–3642. (b) Andrade, C. D.; Yanez, C. O.; Rodriguez, L.; Belfield, K. D. *J. Org. Chem.* **2010**, *75*, 3975–3982.
- (4) Velusamy, M.; Shen, J.-Y.; Lin, J. T.; Lin, Y.-C.; Hsieh, C.-C.; Lai, C.-H.; Lai, C.-W.; Ho, M.-L.; Chen, Y.-C.; Chou, P.-T.; Hisao, J.-K. *Adv. Funct. Mater.* **2009**, *19*, 2388–2397.
- (5) (a) Zhou, G.; Wong, W.-Y.; Poon, S.-Y.; Ye, C.; Lin, Z. *Adv. Funct. Mater.* **2009**, *19*, 531–544. (b) Charlot, M.; Izard, N.; Mongin, O.; Riehl, D.; Blanchard-Desce, M. *Chem. Phys. Lett.* **2006**, *417*, 297–302.
- (6) (a) Yang, Y.; Farley, R. T.; Steckler, T. T.; Eom, S.-H.; Reynolds, J. R.; Schanze, K. S.; Xue, J. *Appl. Phys. Lett.* **2008**, *93*, No. 163305. (b) Goudreaux, T.; He, Z.; Guo, Y.; Ho, C.-L.; Zhan, H.; Wang, Q.; Ho, K. Y.-F.; Wong, K.-L.; Fortin, D.; Yao, B.; Xie, Z.; Wang, L.; Kwok, W.-M.; Harvey, P. D.; Wong, W.-Y. *Macromolecules* **2010**, *43*, 7936–7949. (c) Lincker, F.; Kreher, D.; Attias, A.; Do, J.; Kim, E.; Hapiot, P.; Lemaitre, N.; Gettroy, B.; Ulrich, G.; Ziessel, R. *Inorg. Chem.* **2010**, *49*, 3991–4001.
- (7) (a) Huang, F.; Chem, K.; Yip, H.; Hau, S. K.; Acton, O.; Zhang, Y.; Luo, J.; Jen, A. K.-Y. *J. Am. Chem. Soc.* **2009**, *131*, 13886–13887. (b) Zou, Y.; Najari, A.; Berrouard, P.; Beaupre, S.; Aich, B. R.; Tao, Y.; Leclerc, M. *J. Am. Chem. Soc.* **2010**, *132*, 5330–5331.
- (8) (a) Kono, T.; Kumaki, D.; Nishida, J.; Tokito, S.; Yamashita, Y. *Chem. Commun.* **2010**, *46*, 3265–3267. (b) Le, Y.; Nitani, M.; Kawahara, M.; Tada, H.; Aso, Y. *Adv. Funct. Mater.* **2010**, *20*, 907–913.
- (9) Sakamoto, R.; Kume, S.; Nishihara, H. *Chem.—Eur. J.* **2008**, *14*, 6978–6986.
- (10) Sakamoto, R.; Murata, M.; Nishihara, H. *Angew. Chem., Int. Ed.* **2006**, *45*, 4793–4795.
- (11) (a) Fang, C. S.; Bergmann, W. J. *Org. Chem.* **1951**, *16*, 1231–1237. (b) Begley, M. J.; Crombie, L.; Griffiths, G. L.; Jones, R. C. F.; Rahmani, M. J. *Chem. Soc., Chem. Commun.* **1981**, 823–825. (c) Bowden, K.; Etemadi, R.; Ranson, R. J. *J. Chem. Soc., Perkin Trans. 2* **1991**, 743–746. (d) Irikawa, H.; Adachi, N. *Heterocycles* **2000**, *53*, 135–142. (e) Hashimoto, H.; Shiratori, K.; Kawakita, K.; Tanaka, T.; Sekine, R.; Irikawa, H. *Heterocycles* **2005**, *65*, 1385–1392. (f) Kawabe, C.; Kawakita, K.; Morinaga, M.; Kondo, M.; Irikawa, H. *Heterocycles* **2007**, *71*, 1991–2001. (g) Norsten, T. B.; Kantchev, E. A. B.; Sullivan, M. B. *Org. Lett.* **2010**, *12*, 4816–4819.
- (12) (a) Yamaguchi, S.; Tamao, K. *Chem. Lett.* **2005**, *34*, 2–7. (b) Yamaguchi, S.; Xu, C.; Okamoto, T. *Pure Appl. Chem.* **2006**, *78*, 721–730. (c) Fukazawa, A.; Yamaguchi, S. *Chem.—Asian J.* **2009**, *4*, 1386–1400.
- (13) Albani, J. R. *Structure and Dynamics of Macromolecules: Absorption and Fluorescence Studies*; Elsevier: Amsterdam, 2004.